American Journal of Nanomaterials, 2019, Vol. 7, No. 1, 1-9
Available online at http://pubs.sciepub.com/ajn/7/1/1
Published by Science and Education Publishing
DOI:10.12691/ajn-7-1-1

Biosynthesis of $Zn_5(CO_3)_2(OH)_6$ from Arachis Hypogaea Shell (Peanut Shell) and Its Conversion to ZnO Nanoparticles

M.T. Dieng[1], B.D. Ngom[1,2,3,*], P.D. Tall[1], M. Maaza[2,3]

[1]Laboratoire de Photonique Quantique d'Energie et de NanoFabrication, Faculté des Sciences et Techniques, Université Cheikh Anta Diop de Dakar (UCAD) B.P. 5005 Dakar-Fann Dakar, Sénégal
[2]UNESCO-UNISA Africa Chair in Nanosciences-Nanotechnology, College of Graduate Studies, University of South Africa, Muckleneuk ridge, PO Box 392, Pretoria-South Africa
[3]Nanosciences African Network (NANOAFNET), iThemba LABS-National Research Foundation, 1 Old Faure road, Somerset West 7129, PO Box 722, Somerset West, Western Cape Province, South Africa
*Corresponding author: bdngom@gmail.com

Received January 17, 2019; Revised March 19, 2019; Accepted April 04, 2019

Abstract We report on the novel green biosynthesis of Hydrozincite ($Zn_5(CO_3)_2(OH)_6$) from peanut shell water exacted dye and its conversion to Zincite (ZnO). The structural, morphology and thermogravimetric properties of the as synthesized nanopowders were analyzed using X-ray diffraction (XRD), Fourier Transform Infrared Spectroscopy(FTIR), Raman spectroscopy, Scanning Electron Microscopy (SEM) and TG/DTA thermal analysis. The XRD pattern confirmed the formation of Hydrozincite. The correlations of the results from different techniques confirm the formation of hydrozincite and its conversion to Zincite after heat treatment. The obtained ZnO powders are composed of nanoparticles which are well crystalline with a grain size of 31.11 nm.

Keywords: *hydrozincite, ZnO nanoparticles, biosynthesis, dyes, characterization and physical properties*

Cite This Article: M.T. Dieng, B.D. Ngom, P.D. Tall, and M. Maaza, "Biosynthesis of $Zn_5(CO_3)_2(OH)_6$ from Arachis Hypogaea Shell (Peanut Shell) and Its Conversion to ZnO Nanoparticles." *American Journal of Nanomaterials*, vol. 7, no. 1 (2019): 1-9. doi: 10.12691/ajn-7-1-1.

1. Introduction

Nanomaterials represent an important part of the technological advancements of the 21st century as they lead to a set of new interesting physicochemical properties [1,2]. Their economic potentialities are considerable and visible in several applications fields such as oil and gas [3,4], solar energy [5,6], electronics [7], electro-mechanics [8,9,10], the biomedical domain [11,12] etc. This development of nanotechnologies has expanded the sources of nanoparticles with the increased production of oxides nanomaterials with exceptional properties such as ZnO, TiO_2 and Vanadium oxides family etc.

ZnO belongs to the class of metal oxides, which present a special interest due to the fact that they are not only stable under difficult conditions but also generally considered to be safe for humans and animals [13,14,15]. Thus zinc oxide is a semiconductor with attractive properties: the highest piezoelectric effect (e_{33} = 1.2 C/m^2); the highest exciton binding energy (Ei = 60 meV at 300 K); a large band of gap (3.37 eV at 300 K); a shearing modulus (~ 45.5 GPa) higher than ZnSe (18.35 GPa) and GaAs (32.6 GPa) [16]. Its high chemical, thermal and mechanical stability and its aforementioned properties make it attractive for use in solar thermal applications, etc. [17]. It has a very high thermal conductivity (σ= 0.54 W.cm^{-1}.K^{-1}) hence its use in nanofluid technology for heat transfer applications where it competes strongly with metal nanoparticles such as gold, copper, aluminum etc. [18,19,20,21].

However, access to its nanostructures requires the development of adapted methods of production. The main production methods often used are physical (laser ablation, Sputtering; spray pyrolysis, etc.) and chemical (electrochemical reduction, hydrothermal synthesis, etc.) [22-27]. The major disadvantage in the physical method is the low yield and in the chemical method is the use of toxic solvents. These physicochemical methods are also very costly and potentially dangerous for the environment. As a result, biosynthesis has received increasing attention due to the growing need to develop environmentally and ecofriendly technology in nanoparticles synthesis. The major advantage of this biological approach is its relative simplicity and its speed in the synthesis of nanoparticles [28,29,30]. It provides high yields, low toxicity, low cost and biocompatibility [31]. Another advantage is that the size of the nanoparticles can also be easily controlled by various parameters such as pH and temperature [32,33,34]. Due to the rich biodiversity of plants, this green synthesis has become a subject of interest throughout the world with different plant species explored recently and evaluated for the synthesis of nanoparticles of zinc oxide. The focus is

then placed on an environmentally-friendly procedure involving the bio-reduction/oxidation of zinc salts by extracts from plants such as: Punica Granatum [35], Ocimum Tenuiflorum [36], Aloe Barbadensis Miller [37], Imperata Cylindrica [38], Moringa Oleifera [39], Aspalathus Linearis [40], Nyctanthes Arbor-Tristis [41]; Cassia Fistula [42], Trachyspermum Ammi [43]; Abrus Precatorius [44]. This green synthesis presents enormous environmental and health benefits including the use of invasive [38] and toxic [44] plants and has enabled the production of zinc oxide nanoparticles with excellent physicochemical properties.

In this study, we report on a novel green biological way for the synthesis of ZnO nanoparticles using Arachis Hypogaea shell (peanut shell) dye water extract as a solvent of Zinc nitrate hydrate. Indeed, Peanut is the sixth crop among the most important oil seeds cultivated in the world with an annual output of 37.1 million tons [45]. Moreover peanut shells represent 20% of dried peanut paste by weight. This means that there is a substantial amount of shell residue left after peanut processing [46]. However most of these residues are arbitrarily incinerated or throw away and this can add to environmental pollution [47] of countries large producers such as China, India, Senegal, etc. It is therefore of great economic and environmental importance to explore the use of peanut shell. Efforts have been made in this direction with its use as a source of fodder for livestock, composting of wet materials, wastewater treatment as insulating board, as well as activated charcoal and ethanol production [48]. However, it contains many functional components, which are safe for humans and which could be of interest to the green synthesis of nanoparticles. It is in this sense that this study aims to synthesize nanoparticles of zinc oxide from dye of peanut shell and studied their main physical properties.

2. Experimental Details

2.1. Preparation of Peanuts Shell Dye Extract

Peanut shells were collected and dried under sunny conditions. They were then grounded to give a fine powder. An amount of 3 g of this powder was dissolved in 150 ml of deionized water (DI-H_2O) and stirred vigorously using a magnetic stirrer for 3 hours to ensure maximum extraction of the bioactive compounds. The resulting aqueous extract was then filtered to remove residual solids.

2.2. Biosynthesis of ZnO Nanoparticles

In 100 ml of the peanut shell extract, 0.3 g of $Zn(NO_3)_2.6H_2O$ (zinc nitrate hexahydrate) is dissolved therein. This solution after being magnetically stirred for 1 hour, was then placed in laboratory oven at 300°C for 3 hours to ensure the evaporation of water. Then a brown powder was obtained. This brown powder was divided into three parts: P1, P2 and P3. P1 was not subjected to heat and was taken as a reference sample, P2 was heated for 3h and Finally P3 was heated for 4h, all of them at 500°C in an open-air oven.

2.3. Characterization of ZnO Nanoparticles

X-ray diffraction (XRD) spectra of the as-prepared ZnO powders were collected using a diffractometer (Brucker D8 Advance) with theta/2theta geometry, operating with a copper tube at 50 kV and 30 mA and reflection geometry at 2θ values ranging from 10–90° with a step size of 0.01°. Raman spectroscopy measurements were obtained using a T64000 micro-Raman spectrometer (HORIBA Scientific, Jobin Yvon Technology) with a 514 nm laser wavelength and spectral acquisition time of 120 s was used to characterize the as-prepared samples powders. The FTIR was employed to complete the structural investigation using an ALPHA BRUKER, Platinum ATR, the experimental was done in air. The morphology of the as-prepared powders was studied using a high-resolution Zeiss Ultra Plus 55 field emission scanning electron microscope (FE-SEM) operated at a voltage of 2.0 kV. Thermal properties were characterized using thermal gravimetric analysis (TGA, Q50, TA, New Castle, DE, USA).

3. Results and Discussions

The X-ray diffraction patterns (XRD) of the as prepared and annealed powders are shown in Figure 1. Figure 1a shows the X-ray diffraction pattern of the as prepared powders sample P1. The peaks indexed in the spectrum are closely associated with the powder diffraction JCPDS data for hydrozincite $[Zn_5(CO_3)_2(OH)_6]$ (JCPDS number 00-019-1458 and 01-072-1100) as reported in Table 1. In Figure 1b were is shown the diffraction pattern of sample P2, the presence of less but very intense and well defined diffraction peaks is observed compare to sample P1. These peaks were observed at angle of $2\theta(^o)$ ranging from 28.55 to 89.62 (ref Table 2). According to the standard XRD pattern, the annealed powders (P2) can be indexed as the hexagonal wurtzite structure of ZnO as per predicted with crystallographic orientation directed growth (JCPDS number 36-1451) as reported in Table 2. Also it is noted that the intensities of the Bragg peaks of the P2 sample were sharp and narrow compared with the P1. The Debye-Scherrer approximation makes it possible to estimate the average size of the crystalline grains of P2, which was found to be 31.11 nm as compared to 25.15 nm for P1 (see Table 1 and Table 2). It can therefore be said that the annealing of the sample resulted in the formation of ZnO nanoparticles with excellent crystallinity and increased particle size [49,50]. The peak at $2\theta(^o)$ = 23.76 shown in the diffraction profile of P2 belongs to Hydrozincite and confirms that after 3hours annealing in air we still have hydrozincite in the powder. Figure 1c shows the obtained diffractions peaks from P3 which belonging to pure hexagonal Zinc Oxide, which shows the complete conversion of Hydrozincite to Zincite after 4h of annealing in air at 500°C.

Figure 2 shows the SEM images at different magnifications of the morphology of the biosynthesized powders. The visual reading of the images clearly shows the formation of agglomerated particles having hexagonal shapes with a high yield (Figure 2 (a,b,c)). These nanodisks-like stractures have polished surfaces devoid of

asperities thus promoting their surface properties [51,52]. We observe a multi-structuration during their growth leading to a policrystallization according to different planes as reported on the XRD results and to the different sizes of the grains (Figure 1a and Table 1). There are also nanograins, which tend to coalesce in a given direction whose extremity forms a hexagonal structure thus giving ZnO nanoplates. After 4h of annealing in air at 500°C the morphology of the powders have changed to spherical-like nanoparticles corresponding to the conversion of the nanoplates like structures to nanoparticles (Figure 2d).

Figure 3 reports on the room temperature Raman spectroscopy of the synthesized nanopowders. Figure 3 (a) shows the spectrum of the P1 sample. We observe the appearance of peaks at position around 62, 98, 102, 145, 730, 1050 cm^{-1}. The observed peak at 102 cm^{-1} can be ascribed to the E_2 (Low) of hexagonal crystal structure of ZnO complex, the peak at 145 cm^{-1} could be related to local vibrational modes associated with intrinsic lattice defects while the peak at 730 cm^{-1} is assigned to A_1 (TO) transversal optical mode of ZnO [53]. We assign the mode at 1050 cm^{-1} to A_1 (TO+LO) combinations at the A and H points according to the group theory. Raman microscopy showed vibration modes for the nanopowders for sample P2 and P3 (Figure 3 (b, c)) around: 98, 203, 335, 388 and 437 cm^{-1} assigned to E_2 (Low), $2(A_1(TA) + E_2$ (low)), $3E_2$ (H)–E_2 (L), A_1(TO) and E_2 (high) respectively for ZnO. The peak at 583 cm^{-1} corresponding to A_1 (LO) is correlated with vacancies of oxygen in ZnO, and the others two peaks at 1054 and 1144 cm^{-1} are due to A_1(TO+LO) combinations at the A and H points and to E_1 (2LO) respectively [54,55,56]. After annealing at 500°C (Figure 3 b and c), the E_2 (high) mode appears, and the peak at 142 cm^{-1} related to local vibrational modes associated with intrinsic lattice defects disappears which evidence a better crystalline quality of the ZnO nanopowders with the heat treatment. These results confirm the formation of highly crystalline ZnO after the annealing from the decomposition of $Zn_5(CO_3)_2(OH)_6$ as reported by the XRD results.

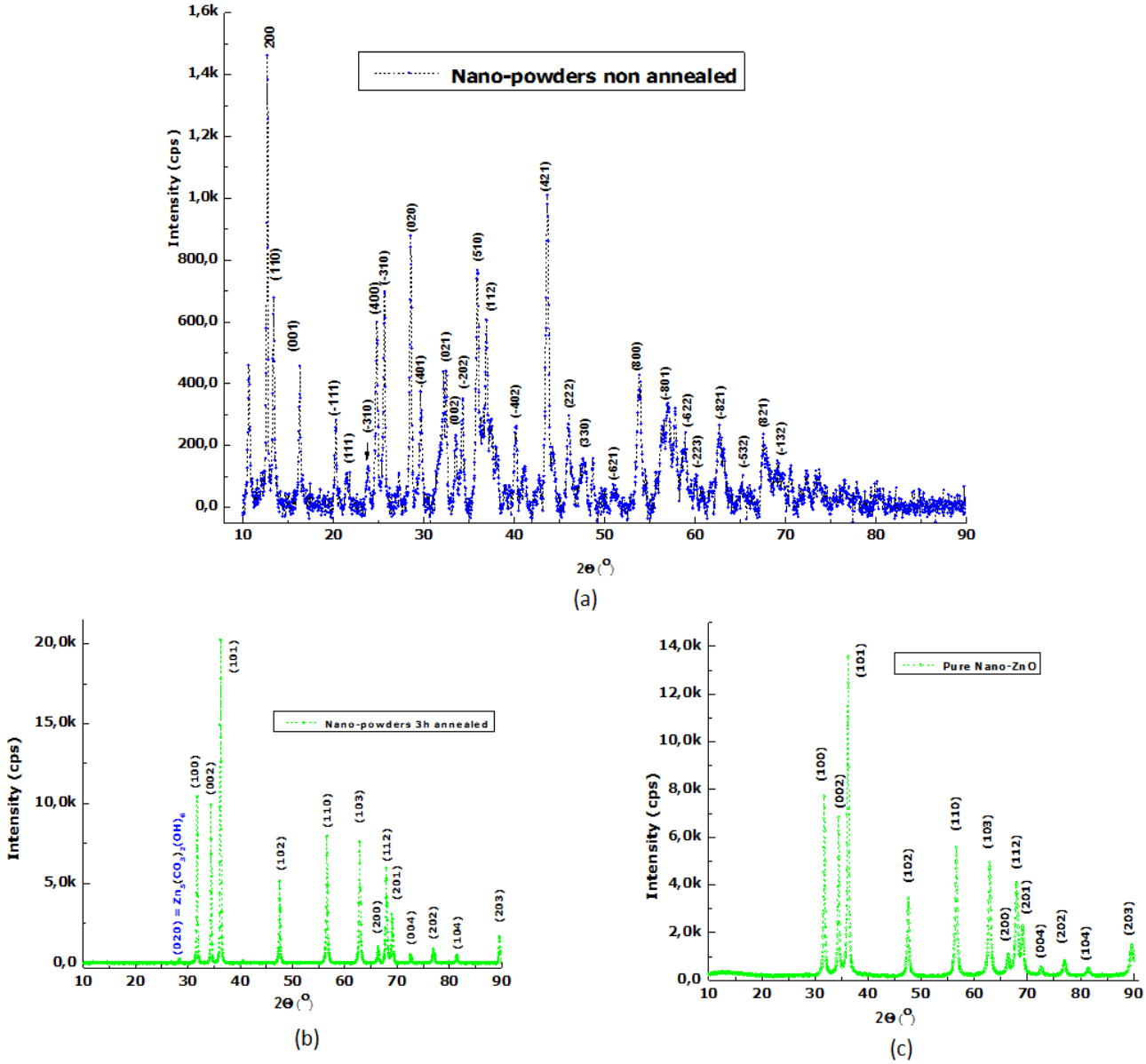

Figure 1. XRD patterns curves of ZnO nanopowders (a) Sample P1: not annealed and (b) Sample P2: Annealed at 500 °C for 3h in air (c) Sample P3: Annealed at 500°C for 4h in air

Table 1. d-spacing, FWHM and Crystallite Size of the nanopowders of the Sample P1: non-annealed sample.

Pos. [°2Th.]	Plan [hkl]	FWHM [°2Th.]	d-spacing [Å]	σ(nm)
10.6881	*	0.5353	8.27750	150
12.9958	200	0.8029	6.81235	100
16.3438	001	0.4015	5.42362	201
20.2702	-201	0.4015	4.38104	202
21.5607	*	0.4015	4.12164	202
23.7578	111	0.3346	3.74523	244
25.6601	*	0.4015	3.47173	204
27.3671	*	0.3346	3.25894	245
28.5609	020	0.4015	3.12538	206
29.7206	-401	0.4015	3.00602	205
32.3986	401	0.5353	2.76340	155
34.0301	-202	0.8029	2.63456	104
35.9535	*	0.3346	2.49791	251
38.2727	-511	0.4015	2.35171	210
38.9386	420	0.3346	2.31302	253
40.2356	-402	0.3346	2.24140	254
41.1744	511	0.3346	2.19244	255
43.7084	421	0.3346	2.07103	257
44.3721	022	0.3346	2.04158	257
46.0405	-131	0.3346	1.97141	259
47.9614	330	0.5353	1.89684	163
48.7398	*	0.3346	1.86836	262
50.9615	003	0.4015	1.79200	220
53.9024	-113	0.7360	1.70097	121
57.0095	-712	0.3346	1.61542	271
58.8413	801	0.4015	1.56943	228
60.1738	240	0.3346	1.53783	275
61.8826	-8O2	0.5353	1.49940	173
62.6224	223/ 820	0.5353	1.48346	174
65.2302	440	0.5353	1.43032	177
66.2545	821	0.4015	1.41067	237
67.5154	513 / -404	0.6691	1.38736	143
69.0613	-713	0.4015	1.36004	241
70.5477	-333	0.3346	1.33498	292
72.3037	114 / -404	0.3346	1.30683	295
73.4744	640	0.6691	1.28887	148
74.6073	-641	0.3346	1.27208	299
76.6399	1020	0.5353	1.24333	190
77.9857	713	0.4015	1.22521	255
80.0511	-913	0.3346	1.19872	311
82.3159	931/ -1022	0.4015	1.17138	263
84.9099	-443/-152	0.5353	1.14210	202
88.9634	823	0.4896	1.09936	228

Table 2. d-spacing, FWHM and Crystallite Size of the nanopowders of the Sample P2: annealed sample at 500°C for 3h in air

Pos. [°2Th.]	Plan [hkl]	FWHM [°2Th.]	d-spacing [Å]	σ(nm)
28.3802	020	0.4015	3.14486	125
31.7713	100	0.4015	2.81651	112
34.4396	002	0.4015	2.60416	104
36.2620	101	0.4015	2.47736	98
40.5876	-402	0.4015	2.22277	88
47.5621	102	0.4015	1.91183	75
56.6195	110	0.3346	1.62562	63
62.9004	103	0.4015	1.47757	57
66.3902	200	0.3346	1.40812	54
67.9635	112	0.3346	1.37930	52
69.0853	201	0.3346	1.35962	52
72.6417	114/-404	0.4015	1.30158	49
76.9341	202	0.4015	1.23931	46
81.3621	104	0.4080	1.18172	44

Table 3. d-spacing, FWHM and Crystallite Size of the nanopowders of the Sample P2: annealed sample at 500°C for 4h in air

Pos. [°2Th.]	Plan [hkl]	FWHM [°2Th.]	d-spacing [Å]	σ(nm)
31.7678	100	0.5353	2.81682	112
34.4154	002	0.8029	2.60594	103
36.2553	101	0.5353	2.47781	98
47.5556	102	0.5353	1.91208	75
56.5931	110	0.8029	1.62632	63
62.8941	103	0.5353	1.47770	57
66.2814	200	0.5353	1.41016	54
67.9708	112	0.5353	1.37917	52
69.1268	201	0.5353	1.35891	52
72.6196	004	0.5353	1.30192	49
76.9966	202	0.6691	1.23846	46
81.4509	104	0.6528	1.18065	44

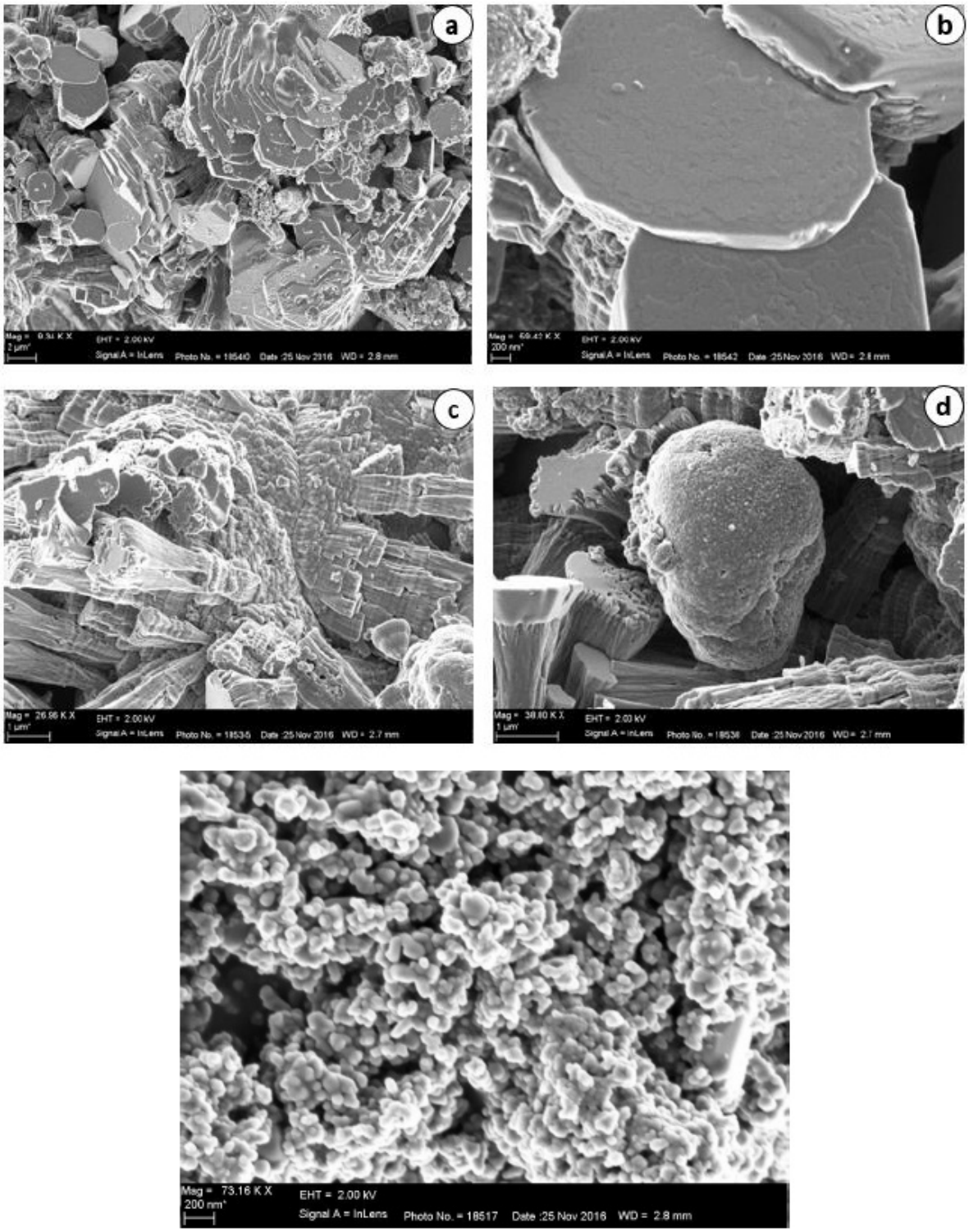

Figure 2. SEM images of ZnO nanopowders; Sample P2: annealed at 500°C for 3h with various magnifications: (a) showing formation of nanodiscs (b) Polished surface with hexagonal nanochip shape (c) Policrystallization during growth (d) ZnO growth mode (e) and Sample P#: ZnO nanoparticles obtained after annealing at 500 °C for 4h in air

The functional groups of samples nanoparticles were analyzed through FTIR spectrum. Figure 4 shows the FTIR spectrum of the biosynthesized nanopowders before and after annealing in air. In the FTIR spectra of P1 sample (Figure 4a), a series of absorption peaks in the range of 500 to 4000 cm-^{1} can be found, corresponding to the basic features of zinc carbonate and hydroxyl groups. To be more specific, the broad peak at 3215 cm^{-1} is assigned to the O-H stretching vibration mode of O-H group. The main peaks observed at 1332, 1420, 1545 and 1655 cm-^{1} are assigned to different carbonate species. The peaks located at 1332, 1420, 1545 and 1655 cm^{-1} are attributed to the adsorption of free CO_3^{2-} species or to antisymmetric O-C-O stretching vibrations. These free CO_3^{2-} species can be associated with vibration bands at 1055, 802 and 730 cm^{-1}, which correspond to the v_1 symmetry, v_2 out-of-plane mode and v_4 in-plane mode, respectively, which are characteristic of the $Zn_5(CO3)_2(OH)_6$ as formed [57,58].

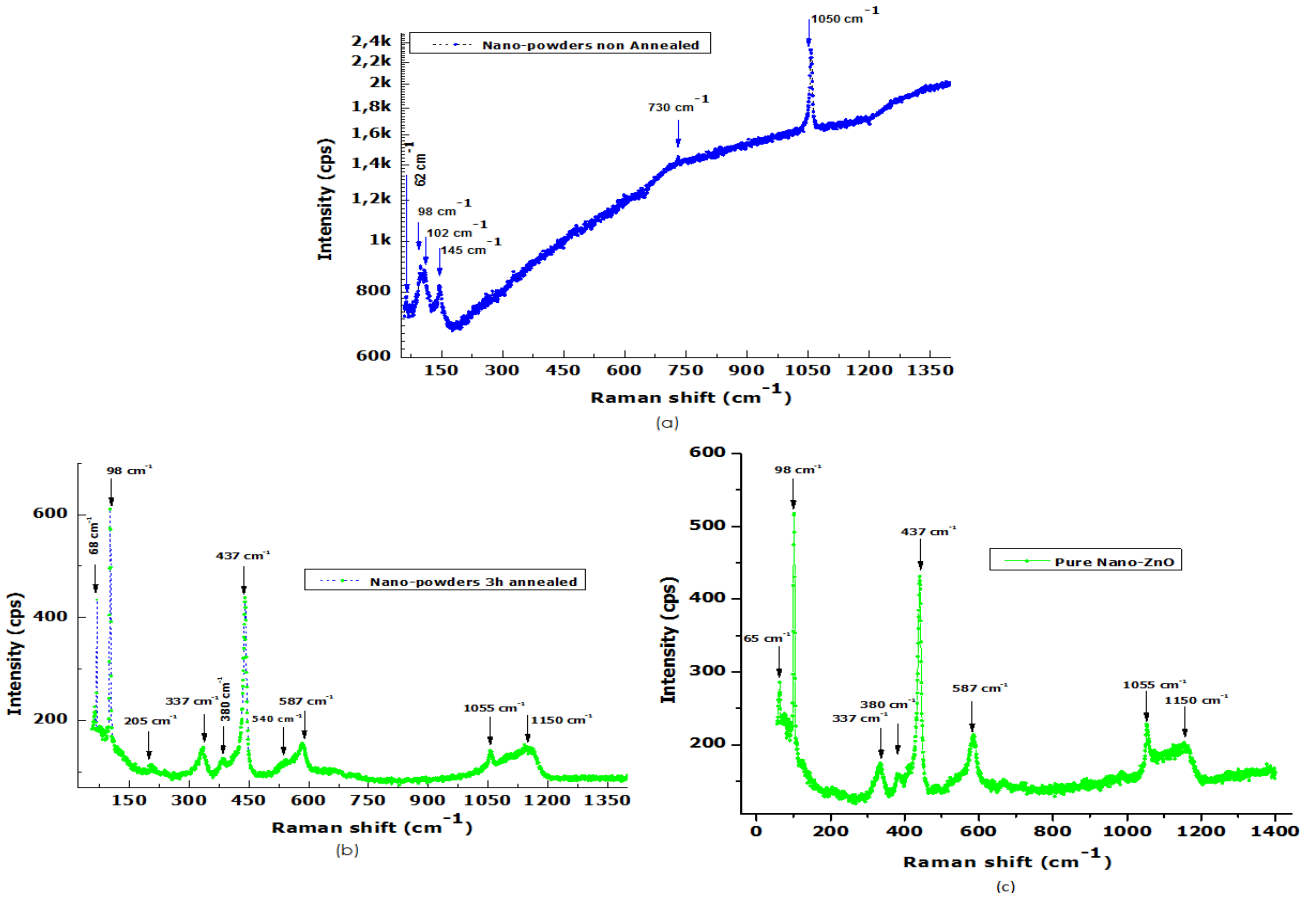

Figure 3. (a) Raman spectrum of Sample P1: non-annealing ZnO nanopowders (b) Raman spectrum of Sample P2: ZnO nanoparticles at 500°C for 3h in air (c) Sample P3: ZnO nanoparticles obtained after annealing at 500°C for 4h in air

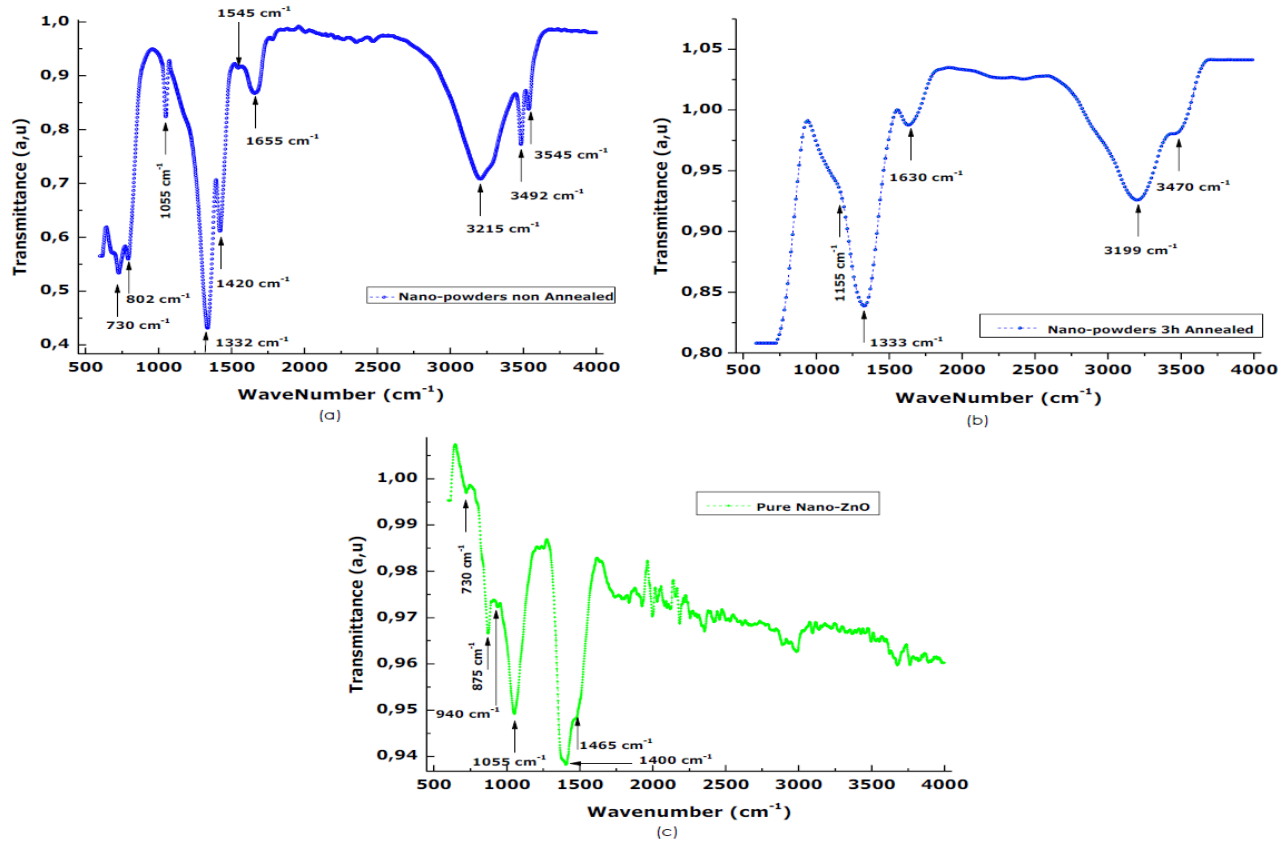

Figure 4. FTIR of ZnO nanopowders (a) Sample P1: not annealed and (b) Sample P2: Annealed at 500°C for 3h in air, (c) Sample P3: ZnO nanoparticles obtained after annealing at 500°C for 4h in air

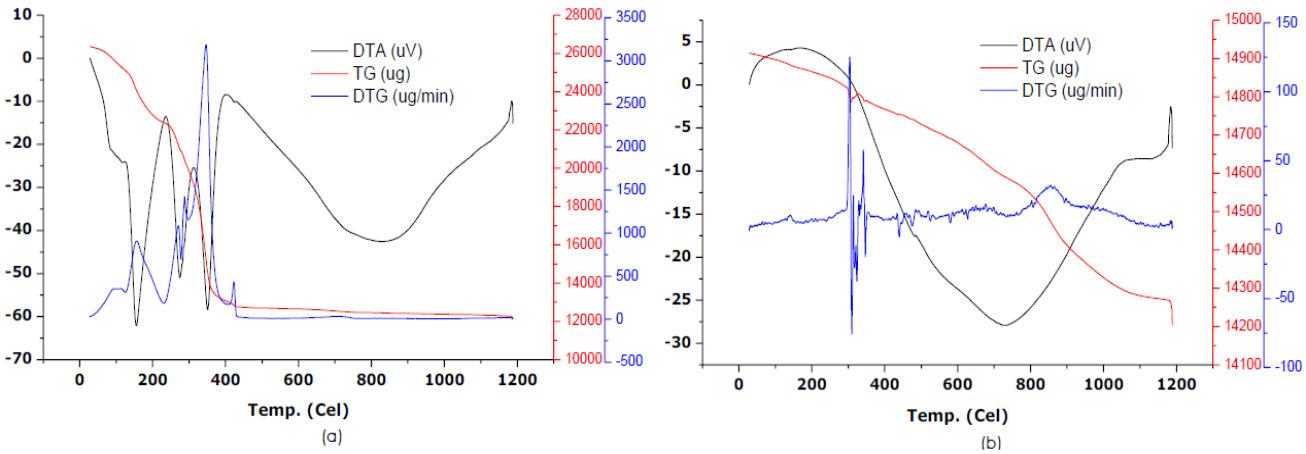

Figure 5. TG-DTG and DTA curves of ZnO nanopowders (a) Sample P1: not annealed and (b) Sample P2: Annealed at 500°C for 3h

When the Hydrozincite is annealed at 500°C for 3h (Figure 4b), the content of the carboxylate (COO-) and hydroxyl (-OH) groups in the samples decreased because their broad peaks became small and shifted towards lower wavenumbers. This indicating the possible dissociation of zinc carboxylate and conversion to ZnO during annealing.

Annealing at 500°C for 4 hours, significantly reduces the carboxylate and remove hydroxyl groups as shown in Figure 4c. Whereas the stretching of ZnO NPs are expected at 730, 875 and 940 cm^{-1}, the FT-IR spectra reveal peak at 1400 and 1055 cm^{-1} which may be assigned respectively to the symmetric stretching of the carboxyl side groups in the amino acid residues of the protein molecules and The band to C–N stretching vibration of amine [59]. No significant absorption peaks at higher wavenumbers are revealed, indicating the nature of the formed ZnO nanoparticles.

The TG-DTG/DTA curves of the biosynthesized samples-NPs are presented in Figure 5. In Figure 5a, corresponding to the P1 sample, the profile of the TGA curve (red line) shows a continuous weight loss with 5 near-sharp changes occurring at 154, 267, 288, 343 and 421°C followed by an almost constant plateau. The peak around 154°C can be attributed to the removal of water, crystallization or evaporation of surface-active molecules adsorbed on the surface of zinc-based complexes during phase solubilization [60,61]. The mass losses accruing around 267 and 288°C can be attributed respectively to the sublimation of the Zinc complex and its conversion to Zinc oxide [62]. The DTA curve has large exothermic peaks at these temperatures, which can be attributed to the fusion and decomposition process of Hydrozincite and the formation of ZnO, which confirm the Raman, FTIR and XRD results. The loss of mass at the temperature range between 343 and 421°C is very high and the corresponding DTA curve shows two important exothermic peaks. This could be attributed to the formation of zinc oxide nanoparticles and the decomposition of carbonates [63]. When the temperature reached above 421°C, no other weight loss was observed. This indicates that the entire reaction process ends with the formation of ZnO nanocrystalline. Hence, annealing above 421°C appears to ensure the formation of stable ZnO nanoparticles. Figure 5b shows the thermal behavior of the ZnO nanoparticles obtained after annealing at 500°C for 3h. It can be seen that the weight losses throughout the temperature range are relatively small in contrast to Figure 5a. Those observed in the temperature ranges of 200 to 400°C are due to the volatilization of the combustible carbonates species present in the sample. The endothermic peak of the DTA curve at 750°C is due to the increase of crystallization rate with increasing temperature [64,65]. This shows the high stability of the ZnO nanoparticles in the measured temperature range.

4. Conclusion

The novel green biosynthesis method was successfully used to synthesis a well crystalline ZnO nanoparticles from the peanut shell water exacted dye. The structural analysis results confirm that indeed the synthesized nanoparticles are of a high quality ZnO. These nanoparticles have the disk-like morphology as seen from the SEM results. The correlations of the results from different techniques confirm the formation of hydrozincite and its conversion to Zincite after heat treatment leads to the ZnO nanoparticles, which are well crystalline with a grain size of 31.11 nm.

Acknowledgments

This work was supported by the TWAS-UNESCO Associate Scheme through the University of South Africa (UNISA) as a host institution. The TWAS-UNESCO Associate holder Prof BD Ngom is very thankful to the TWAS-UNESCO as well as the host institution. We are also thankful to iThemba LABS-National Research Foundation of South Africa and the University of Pretoria for the use of their facilities.

References

[1] Lahmani M, Bréchignac C Les Potentialités Economiques Importantes De Ces Nouvelles Technologies Et Leurs, Houdy P ; Les Nanosciences 2.Nanomatériaux Et Nanochimie, 2e Edition, Edition Belin; 2012.

[2] Pascale LAUNOIS, Nanosciences Et Nanotechnologies, Rapport De Conjoncture, 2004.

[3] Franco, C.A., Zabala, R., Cortés, F.B., Nanotechnology Applied To The Enhancement Of Oil And Gas Productivity And Recovery

Of Colombian Fields, *Journal Of Petroleum Science And Engineering* (2017).

[4] Lau, H.C., Yu, M., Nguyen, Q.P., Nanotechnology For Oilfield Applications: Challenges And Impact, *Journal Of Petroleum Science And Engineering* (2017).

[5] Ahmed Kadhim Hussein, Applications Of Nanotechnology To Improve The Performance Of Solar Collectors – Recent Advances And Overview, Renewable And Sustainable Energy Reviews Volume 62, September 2016, Pages 767-792.

[6] Z. Abdin, M.A.Alim, R.Saidur, M.R.Islam, W.Rashmi, S.Mekhilef A.Wadi, Solar Energy Harvesting With The Application Of Nanotechnology, Renewable And Sustainable Energy Reviews, 2013.

[7] Yaser Dahman, Electronic And Electro-Optic Nanotechnology, Nanotechnology And Functional Materials For Engineers**,** A Volume In Micro And Nano Technologies**,** 2017, Pages 191-206.

[8] J.E. Contreras, Et Al., Nanotechnology Applications For Electrical Transformers—A Review, Electr. Power Syst. Res. (2016).

[9] L. Lundgaard, W. Hansen, D. Linhjell, T.J. Painter, Aging Of Oil-Impregnatedpaper In Power Transformers, IEEE Trans. Power Deliv. 19 (2004) 230-239.

[10] J.H. Harlow, Electric Power Transformer Engineering, CRC Press, 2004.

[11] Hafaid Imen, Etudes Physico-Chimique De Capteur A Base De Nanomatériaux Pour Des Applications Biomédicale, Thèse, INSA LYON, 2009.

[12] Bashir Ahmad, Nabia Hafeez, Shumaila Bashir, Abdur Rauf, Mujeeb-Ur-Rehman, Phytofabricated Gold Nanoparticles And Their Biomedical Applications, Biomedicine & Pharmacotherapy 89 (2017) 414-425.

[13] Melanie Auffan, Nanoparticules D'oxydes Métalliques: Relations Entre La Réactivité De Surface Et Des Réponses Biologiques, Thèse De Doctorat, 2007.

[14] Stoimenov P.K., K.R.L., Marchin G.L. And Klabunde K.J., *Metal Oxide Nanoparticles As Bactericidal Agents.* Langmuir, 2002. **18**: P. 6679-6686.

[15] Fu L., L.Z., Liu Y., Han B., Hu P., Cao L. And Zhu D., *Beaded Cobalt Oxide Nanoparticles Along Carbon Nanotubes: Towards More Highly Integrated Electronic Devices.* Advanced Materials, 2005. **17**: P. 217-221.

[16] S.J. Pearton, D.P. Norton, K. Ip, Y.W. Heo And T. Steiner, Recent Progress In Processig And Properties Of Zno, Superlattices And Microstructures, Vol.34 (1-2), Pp. 3-32 (2003).

[17] S.O. Kucheyev, J.E. Bradley, J.S. Williams, C. Jagerdish, M.V. Swain, Effect Of High-Density Plasma Etching On The Optical Properties And Surface Stoichiometry Of Zno, Appl. Phys. Lett. 80 (2002) 956.

[18] Dhinesh Kumar Devendiran, Valan Arasu Amirtham, A Review Onpreparation, Characterization, Properties And Applications Of Nanofluids, Renewable And Sustainable Energy Reviews, 2016.

[19] Khanna PK; Study Of Zinc Oxide Nanofluids For Heat Transfer Application; Article; SAJ Nanoscience And Nanotechnology; 2015.

[20] A. Yadav, V. Prasad, A.A. Kathe, R. Sheela, Y. Deepti, C. Sundaramoorthy, Vigneshwaran, Bull. Mater. Sci. 29 (6) (2006) 641.

[21] R. Lamb, I.I. Zhang, A. Jones, Postle R Proc. 83rd TIWC, Shanghai, China, (2004), P. 682.

[22] Hatem Moussa; Influence De L'association De Quantum Dots Zno Avec Des Ions Cu2+ Sur Leur (Photo) Toxicité. Nouveaux Matériaux Zno/Rgo Pour La Photocatalyse Solaire ; Thèse De Doctorat ; 2016.

[23] A. Ahmad, P. Mukherjee, S. Senapati, D. Mandal, M. I. Khan, R. Kumar And M. Sastry, *Colloids Surf., B*, 2003, 28, 313-318.

[24] J. Huang, Q. Li, D. Sun, Y. Lu, Y. Su, X. Yang, H.Wang, Y.Wang, W. Shao, H. Ning, J. Hong And C. Chen, *Nanotechnology*, 2007, 18(105), 104.

[25] Z. Hui, Y. Deren, M. Xiangyang, J. Yujie, X. Jin, Q. Duanlin, Nanotechnology 15 (2004) 622.

[26] A. Frattini, N. Pellegri, D. Nicastro, O.D. Sanctis, Matter. Chem. Phys. 94 (2005) 14.

[27] *H. Gleiter*, NANOCRYSTALLINE MATERIALS, *Progress In Materials Science* Vol. 33, Pp. 223-315.

[28] C. Rossignol, J. Dexpert-Ghys, M. Verelst, R. Mauricot, B. Guizard, J.D. Lulewicz, R. Bacsa, P. Serp, N. Reuge, L. Cadoret, B. Caussat, S. Rul, Procedes De Synthese Et De Traitements De Nano Poudres D'oxydes, Conference Paper January 2007.

[29] WILEY Blackwell, Bio-Nanoparticles: Biosynthesis And Sustainable Biotechnological Implications, Edited By Om V. Singh, 2015.

[30] Mahendra Rai And Clemens Posten, Green Biosynthesis Of Nanoparticles: Mechanisms And Applications, CAB International, 2013.

[31] Siavash Iravani, Green Synthesis Of Metal Nanoparticles Using Plants, Green Chem., 2011, 13, 2638.

[32] Kalimuthu, K., Gopalram, S., Vaidyanathan, R., Deepak, V., Pandian, S.R.K. And Gurunathan, S. (2010) Optimization Of A-Amylase Production For The Green Synthesis Of Gold Nanoparticles. Colloids Andsurfaces B: Biointerfaces 77(2), 174-180.

[33] Gurunathan, S., Lee, K.J., Kalishwaralal, K., Sheikpranbabu, S., Vaidyanathan, R. And Eom, S.H. (2009a) Antiangiogenic Properties of Silver Nanoparticles. *Biomaterials* 30, 6341–6350.

[34] Gurunathan, S., Kalishwaralal, K., Vaidyanathan, R., Venkataraman, D., Pandian, S.R.K., Muniyandi, J., *Et Al*. (2009b). Biosynthesis, Purification And Characterization Of Silver Nanoparticles Using *Escherichia Coli*. *Colloids And Surfaces B* 74(1), 328-335.

[35] M. Sundrarajan, S. Jegatheeswaran, S. Selvam, R. Gowri, M. Balaji, K. Bharathi, Green Approach: Ionic Liquid Assisted Synthesis Of Nanocrystalline Zno In Phyto Medium And Their Antibacterial Investigation, *Materials Letters* (2017).

[36] Sagar Raut, Dr. P. V. Thorat, Rohini Thakre, Green Synthesis Of Zinc Oxide (Zno) Nanoparticles Using Ocimum Tenuiflorum Leaves, International Journal Of Science And Research (IJSR) ISSN (Online): 2319-7064, (2013).

[37] Gunalan Sangeetha, Sivaraj Rajeshwari, Rajendran Venckatesh, Green Synthesis Of Zinc Oxide Nanoparticles By Aloe Barbadensis Miller Leaf Extract: Structure And Optical Properties, Materials Research Bulletin, (2011).

[38] I S Saputra And Y Yulizar, Biosynthesis And Characterization Of Zno Nanoparticles Using The Aqueous Leaf Extract Of *Imperata Cylindrica L.*, Materials Science And Engineering31886(2017) 012004.

[39] N. Matinise, X.G. Fuku, K. Kaviyarasu, N. Mayedwa, M. Maaza , Zno Nanoparticles Via Moringa Oleifera Green Synthesis: Physical Properties & Mechanism Of Formation, Applied Surface Science (2017).

[40] A. Diallo, B.D. Ngom, E. Park, M. Maaza, Green Synthesis Of Zno Nanoparticles By Aspalathus Linearis: Structural & Optical Properties, Journal Of Alloys And Compounds (2015).

[41] Jamdagni, P. Et Al., Green Synthesis Of Zinc Oxide Nanoparticles Using Flower Extract Of Nyctanthes Arbor-Tristis And Their Antifungal Activity. Journal Of King Saud University – Science (2016).

[42] D. Suresh, P.C.Nethravathi, Udayabhanu, H. Rajanaika, H. Nagabhushana, S.C. Sharma Green Synthesis Of Multifunctional Zinc Oxide (Zno) Nanoparticles Using Cassiafistula Plant Extract And Their Photodegradative, Antioxidant And Antibacterial Activities, Materials Science In Semiconductor Processing · March 2015.

[43] D. Saravanakkumar1, S. Sivaranjani, M. Umamaheswari, S. Pandiarajan And B. Ravikumar, Green Synthesis Of Zno Nanoparticles Using *Trachyspermum Ammi* Seed Extract For Antibacterial Investigation, Der Pharma Chemica, 2016, 8(7): 173-180.

[44] Kavita Vishwakarma, Green Synthesis Of Zno Nanoparticles Using *Abrus Precatorius* Seeds Extract And Their Characterization, Thesis Of Master Degree, Roll No. 411ls2069,

[45] FAO, CSE, 2003. L'évaluation De La Dégradation Des Terres Au Sénégal. Projet FAO Land Degradation Assessment. Rapport Pré-Liminaire. Avril. 59 P.

[46] Palmer, JM. (2010).The Use Of Peanut By-Products In Stocker Cattle Diets. Page No. 14.

[47] Gutang C. G, Dacua Micah And Deiparine P.S (2012). Peanut (Arachis Hypogaea) Shells And Carton Bulletin Board. Http://Www.Studymode.Com/Essays/Peanut-Shells-1128937.Html.

[48] Priyamwada Bharthare, Preeti Shrivastava, Pushpendra Singh, Archana Ttiwari, Peanut Shell As Renewable Energy Source And Their Utility In Production Of Ethanol, International Journal Of Advance Research, Ijoar .Org, Volume 2, Issue 4, April 2014.

[49] Rajeswari Yogamalar, Ramasamy Srinivasan, Ajayan Vinu, Katsuhiko Ariga, Arumugam Chandra Bose, X-ray peak

broadening analysis in ZnO nanoparticles, Solid State Communications, 2009.

[50] A. Khorsand Zak, W.H. Abd. Majid, M.E. Abrishami, Ramin Yousefi, X-ray analysis of ZnO nanoparticles by WilliamsoneHall and sizeestrain plot methods, Solid State Sciences, 2010.

[51] Lahmani M, Bréchignac C Les Potentialités Economiques Importantes De Ces Nouvelles Technologies Et Leurs, Houdy P ; Les Nanosciences 2.Nanomatériaux Et Nanochimie, 2e Edition, Edition Belin ; 2012.

[52] Y.L. Wu, A.I.Y. Tok, F.Y.C. Boey, X.T. Zeng X.H. Zhang, Surface modification of ZnO nanocrystals, Applied Surface Science, 2017.

[53] U. Haboeck, A. Hoffmann, C. Thomsen, A. Zeuner, and B. K. Meyer High-energy vibrational modes in nitrogen-doped Zn phys. stat. sol. (b) 242, No. 3, R21-R23 (2005).

[54] Aurangzeb Khan, Raman Spectroscopic Study Of The Zno Nanostructures, J Pak Mater Soc 2010.

[55] T. C. Damen, S. P. S. Pqrtq, And B. Tell, Raman Effect In Zinc Oxide, Ph Ysical Review, February 1966.

[56] C. Vargas-Hernández, F. N. Jiménez-García, J. F. Jurado. Comparison of ZnO thin films deposited by three different SILAR processes, Microelectron. J (2008).

[57] O. Aguilar, et al., Novel preparation of ZnS from Zn5(CO3)2(OH)6 by the hydro- or solvothermal method for H2 production, Catal. Today (2016).

[58] R. Wahab, S.G. Ansari, Y.S. Kim, M.A. Dar, H.-S. Shin, Synthesis andcharacterization of hydrozincite and its conversion into zinc oxidenanoparticles, J. Alloys Compd. 461 (2008) 66-71.

[59] S.K. Das, A.R. Das, A.K. Guha, Langmuir 25 (2009) 8192-8199.

[60] Yang Yang, Huilan Chena, Bin Zhao, Ximao Bao, Size Control Of Zno Nanoparticles Via Thermal Decomposition Of Zinc Acetate Coated On Organic Additives, Journal Of Crystal Growth 263 (2004) 447-453.

[61] N. Matinise, X.G. Fuku, K. Kaviyarasu, N. Mayedwa, M. Maaza, Zno Nanoparticles Via Moringa Oleifera Green Synthesis: Physical Properties & Mechanism Of Formation, Applied Surface Science, 2017.

[62] T. Arii, A. Kishi, Thermochim. Acta 400 (2003) 175.

[63] Kalyani Ghule, Anil Vithal Ghule, Bo-Jung Chen And Yong-Chien Ling, Preparation And Characterization Of Zno Nanoparticles Coated Paper And Its Antibacterial Activity Study, The Royal Society Of Chemistry, 2006.

[64] Samira Bagheri, Chandrappa K. G.* And Sharifah Bee Abd Hamid, Facile Synthesis Of Nano-Sized Zno By Direct Precipitation Method, Scholars Research Library, 2013.

[65] Rizwan Wahab, S.G. Ansari, Young Soon Kim, M.A. Dar, Hyung-Shik Shin Synthesis And Characterization Of Hydrozincite And Its Conversion Into Zinc Oxide Nanoparticles, Journal of Alloys and Compounds, 2008.